5. Simulation of the Effects of Predicted and Actual Cam Errors on Valve Train Dynamics

5.1 Objective of the Simulations

In this section, the simulated dynamics of high speed valve trains using cams that vary from the theoretical profile will be presented. Specifically, the following will be looked at:

- Comparison of experimental and simulated results for valve train dynamics using cams generated by the rocker grinder model with grinding wheel size reduction.
- Simulated valve train dynamics using the cam profiles predicted by changes in the rocker length and vertical wheel position of the rocker grinder mechanism.
- Simulated valve train dynamics using cam curves containing actual (measured) errors due to the computer numerical control (CNC) machining process.

The simulations presented herein were performed using the model developed by Kim [30], and as modified by Cheng [31] and Etheridge [32].

5.2 Valve Train Model

The valve train model contains lumped mass models of the cam, lifter, pushrod, rocker arm and valve, along with a finite element model of the valve springs [32]. A schematic of this model is shown in Figure 5.1. The camshaft, rocker arm center pivot shaft, and valve stem are assumed rigid. Coulomb friction acts at the rocker arm center

pivot, valve stem and along each valve spring. Friction in the valve spring nest is due to the presence of a flat steel friction damper installed between the springs. The nonlinear effects of component contact and separation are included by setting corresponding damping and stiffness coefficients to zero during the separation events. By summing forces on masses, m_1 *and* m_3, and moments on the rocker arm with equivalent inertia, I_2, the equations of motion of the valve train excluding the valve springs and seat are derived:

$$m_1 \ddot{y}_1 + (c_1 + c_2)\dot{y}_1 + ac_2\dot{J}_2 + (k_1 + k_2)y_1 + ak_2 J_2 = k_1 d(t) + c_1 \dot{d}(t) \tag{5.1}$$

$$I_2 \ddot{J}_2 + ac_2\dot{y}_1 + (a^2 c_2 + b^2 c_3)\dot{J}_2 - bc_3\dot{y}_3 + ak_2 y_1 + (a^2 k_2 + b^2 k_3)J_2 - bk_3 y_3 = \pm h_{fric} - bk_3 v_{lash} \tag{5.2}$$

$$m_3 \ddot{y}_3 - bc_3\dot{J}_2 + c_3\dot{y}_3 - bk_3 J_2 + (k_3 + k_v)y_3 = f_{spring} \pm f_{fric} + k_3 v_{lash} \tag{5.3}$$

Using helical rod elements the valve springs' equations of motion can be written in the form (32):

$$[M]\{\ddot{\bar{z}}\} + z[K]\{\dot{\bar{z}}\} + [K]\{\bar{z}\} = \{F\} \tag{5.4}$$

where $[M]$ and $[K]$ are the total lumped mass and stiffness matrices, respectively. The boundary conditions for each valve spring are assumed to be fixed at the base and top node with the exception that the vertical displacements of the top node are allowed. The damping in the valve springs is assumed to be a combination of both viscous and Coulomb damping. The viscous damping is assumed proportional to the stiffness matrix. The external force vector $\{F\}$ consists of the valve spring reaction force at the top node and the Coulomb friction force along the valve springs. The retainer, keepers and valve stem are

assumed rigid, hence the vertical displacement of the valve stem is equal to the vertical displacement of each of the top nodal points in each valve spring.

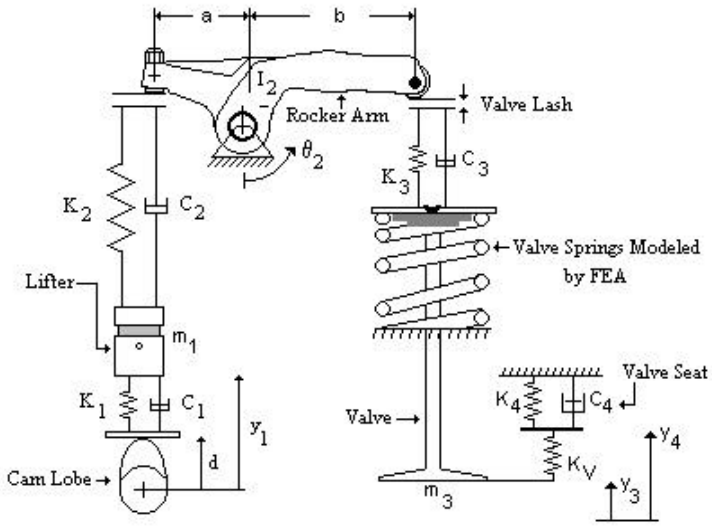

Figure 5.1: Lumped mass and fea model of valve train

The valve head is modeled as an equivalent stiffness determined from a thin-plate analysis with assumed constant thickness. The boundary conditions for the support conditions along the contact edge with the valve seat is assumed as simply supported, hence the equivalent stiffness is given by:

$$k_v = \frac{1.8132\, E_v\, h^3}{r_v^2} \tag{5.5}$$

If the valve is in contact with the valve seat, equation 5.5 is applied to determine the valve head stiffness. If there is no contact, the valve is assumed to be rigid and the stiffness is set equal to zero. The valve seat is modeled with a linear spring and damper. There is no

lumped mass present at the valve seat surface, hence the equation of motion from summing forces at the seat is first order:

$$c_4 \dot{y}_4 = k_v\left(y_3 - y_4\right) - k_4 y_4 \tag{5.6}$$

The complete set of equations of motion for the entire valve train are derived by combining equations 5.1 through equation 5.4 (inclusive) and equation 5.6. In addition, the equations can be manipulated to eliminate the valve spring reaction force from equations 5.3 and 5.4. The results can be written in the form:

$$\{\ddot{\tilde{z}}\} = [\tilde{M}]^{-1}(\{\tilde{F}\} - [\tilde{C}]\{\dot{\tilde{z}}\} - [\tilde{K}]\{\tilde{z}\}) \tag{5.7}$$

Hence, if the cam lift $d(t)$ and velocity $\dot{d}(t)$ profiles are known, equation 5.7 can be integrated to determine the displacement of the valve over a steady state cycle. Steady state response is determined by integrating over multiple cam cycles starting with zero initial conditions until the following condition is satisfied:

$$\sum_{i=1}^{360}\left((y_3^n(i) - y_3^{n-1}(i))^2 + (y_3^{n-1}(i) - y_3^{n-2}(i))^2\right) < 1.0\times10^{-4} \quad for \quad n>4 \tag{5.9}$$

for the $n'th$ cam cycle or until the twentieth cam cycle is reached. The condition presented in equation 5.8 is simply checking the response of valve position. If the sum of the squares of the valve bounce difference matches within the specified tolerance, the system is considered to have reached its steady state response.

The integration routine involves integrating the accelerations of each degree of freedom to obtain the corresponding velocities and positions. The number of equations can vary from approximately 50 to 200 depending upon the number of valve springs in the system, as well as, the number of finite elements required to model the valve springs. Using experimental valve displacement data, (obtained from the experimental procedure previously described in Chapter 4) the required stiffness, damping and friction model parameters were identified using an implicit, filtering algorithm [101].

5.3 Results of Valve Train Simulations for Cam Profiles with Grinding Wheel Diameter Errors

Valve train simulations were performed using both the Comp Cams 938 and K Motion 1600 type springs. Input to the model is the kinematic displacement and velocity of the cam profile. The lift and velocity curves generated in Chapter 3 for grinding wheel diameters of 0.406, 0.305 and 0.203 meters (16, 12 and 8 inches) were used in the simulations to predict changes in valve train dynamics. The simulated results are plotted with the experimental data in Figures 5.2, 5.3 and 5.4 for the Comp Cams 938 and Figures 5.5, 5.6 and 5.7 for the K Motion 1600 for each of the wheel sizes listed above. These figures compare the simulated valve bounce amplitude to the experimentally determined bounce envelope for the original system and the test results for a cam generated using a reduced grinding wheel size. As can be seen in these figures, the bounce amplitude is close to the bounce envelope (if not contained in it). The values that exceed the bounce envelope limit are not out of the acceptable bounce range of 0.254 millimeters (0.010

inches). In addition, the limit speed in each of the figures agrees within 100 rpm which is in the acceptable range of accuracy. Therefore, a good correlation exists between the model and the experimental results to predict valve train dynamics. Based upon these results, the valve train model offers an excellent method of predicting changes in valve train behavior without testing each individual error cam profile.

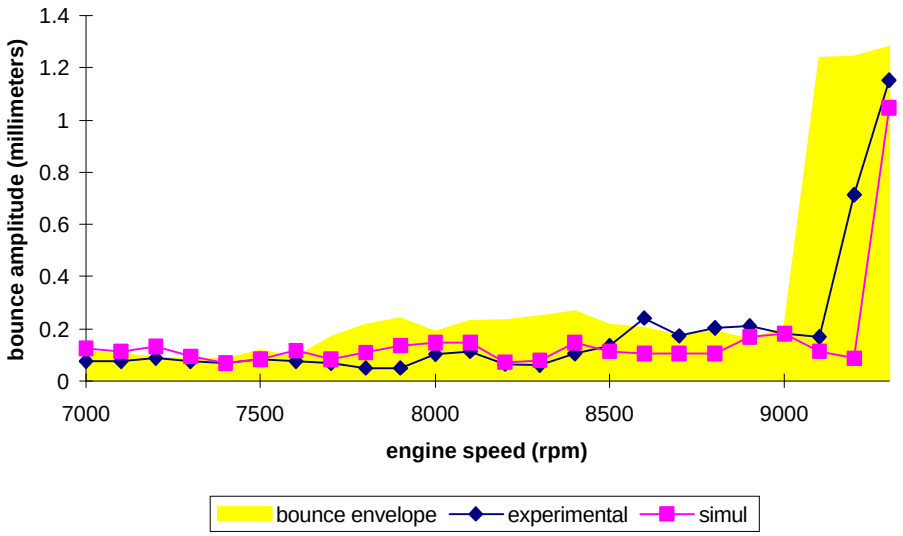

Figure 5.2: Simulated and experimental data for the cam generated using a 0.406 meter (16 inch) grinding wheel using the comp cams 938 spring

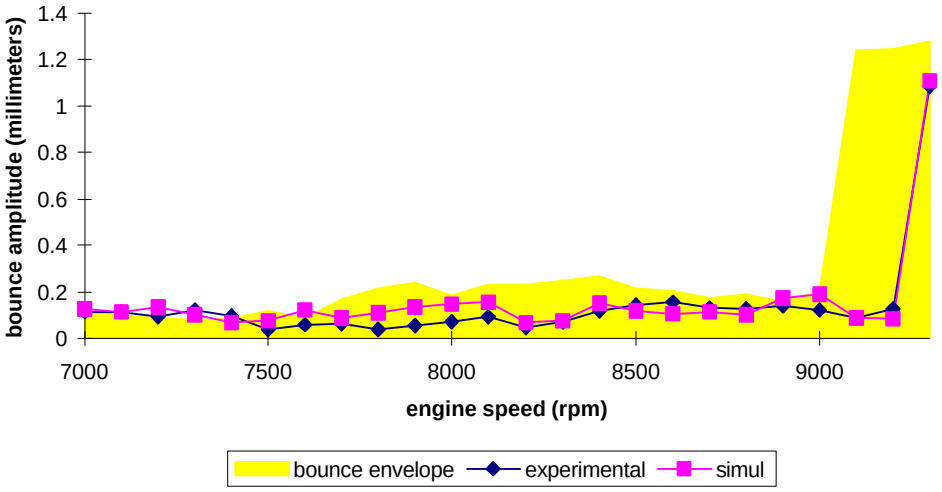

Figure 5.3: Simulated and experimental data for the cam generated using a 0.305 meter (12 inch) grinding wheel and the comp cams 938 spring

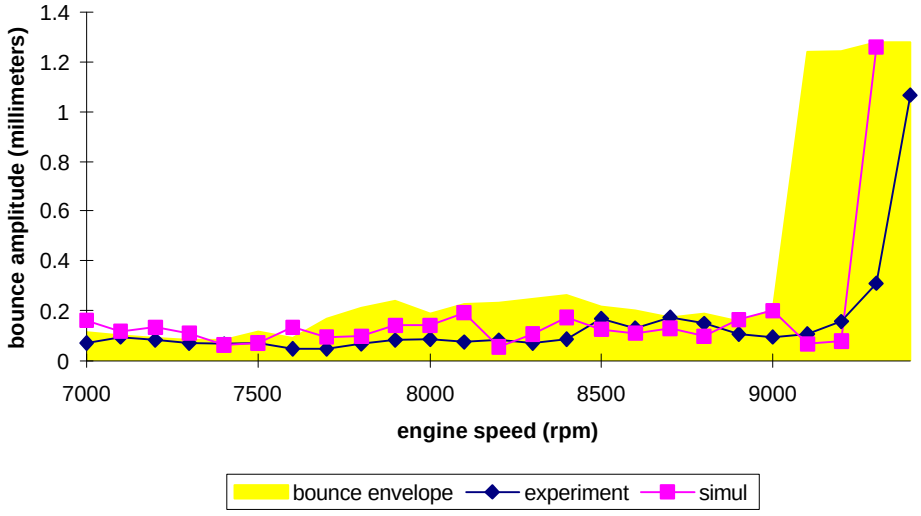

Figure 5.4: Simulated and experimental data for the cam generated using a 0.203 meter (8 inch) grinding wheel and the comp cams 938 spring

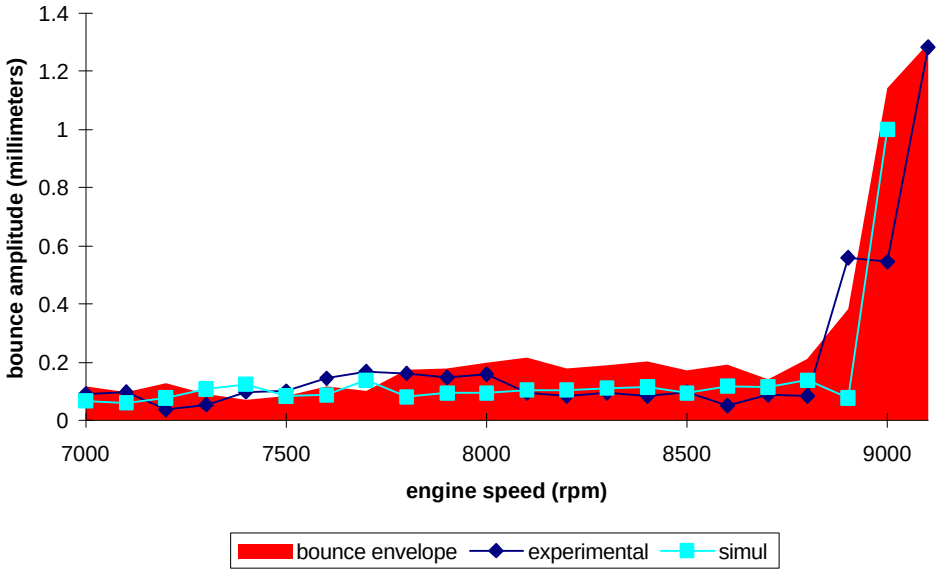

Figure 5.5: Simulated and experimental data for the cam generated using a 0.406 meter (16 inch) grinding wheel and the k motion 1600 spring

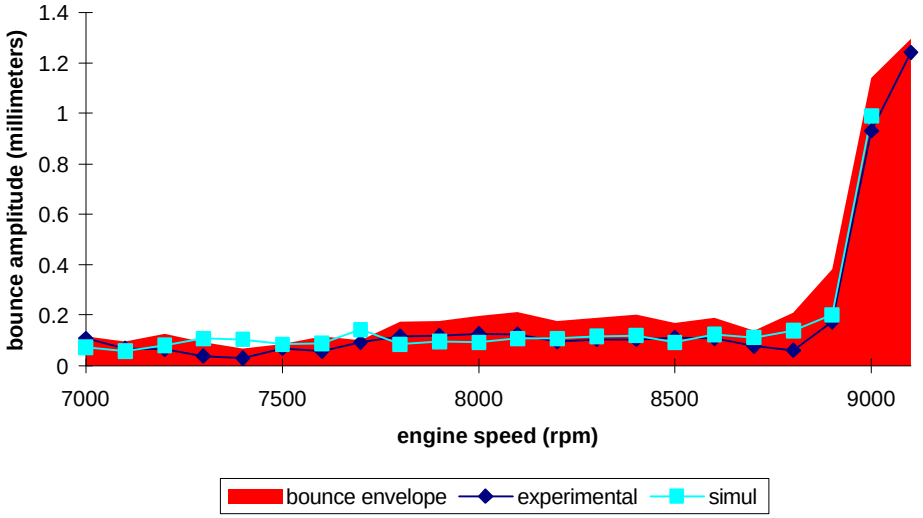

Figure 5.6: Simulated and experimental data for the cam generated using a 0.305 meter (12 inch) grinding wheel and the k motion 1600 spring

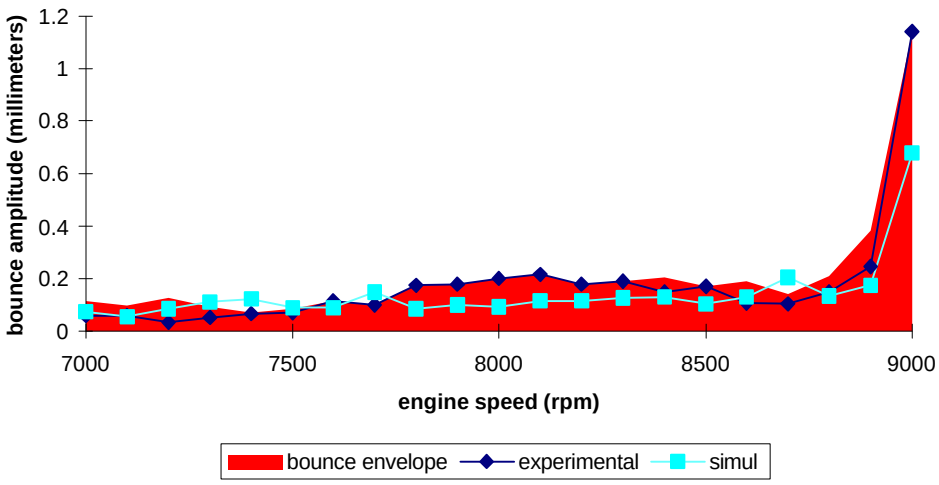

Figure 5.7: Simulated and experimental data for the cam generated using a 0.206 meter (8 inch) grinding wheel and the k motion 1600 spring

5.4 Results of Valve Train Simulations for Cam Profiles with Rocker Length Variation and Vertical Wheel Position Errors

Since the results of the experimental and simulated valve train dynamics correlated well, the cam profiles that were predicted from varying the rocker length and vertical grinding wheel position will be evaluated using the simulation only. Simulations were performed using both spring types used previously in this work: the Comp Cams 938 and the K-Motion 1600. Results for the Comp 938 spring type for the rocker length variation and grinding wheel vertical position are presented in Figures 5.8 and 5.9 respectively. In addition, results for the K Motion spring type for the rocker length variation and grinding wheel vertical position are presented in Figures 5.10 and 5.11 respectively. These figures compare the simulated valve bounce amplitude to the experimentally determined bounce envelope for the theoretical system. As can be seen in the figures, the predicted bounce amplitudes match well with the bounce envelopes. In addition, the limit speeds remain

consistent in the simulation. Moreover, the predictions overlap each other. This shows that these manufacturing errors which result in changes of the lift curve on the order of thousandths of an inch do not effect the dynamics of high speed valve trains significantly. Therefore, if dynamic considerations are of importance in the selection of a valve train, this work indicates that some leeway (on the order of typical shop standards) is available when manufacturing camshafts intended for high speed valve trains.

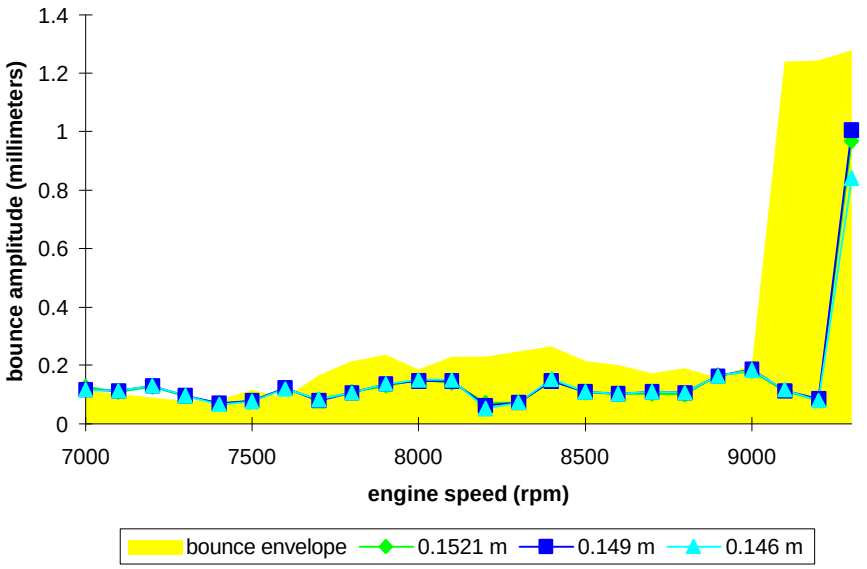

Figure 5.8: Simulated data for the cam generated using various rocker link lengths and the comp cams 938 spring

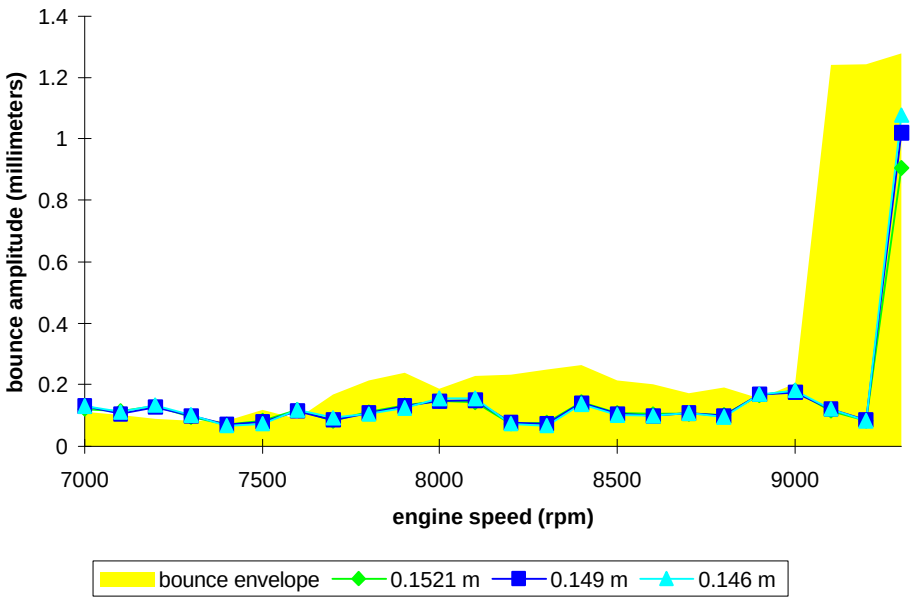

Figure 5.9: Simulated data for the cam generated using various vertical grinding wheel vertical positions and the comp cams 938 spring

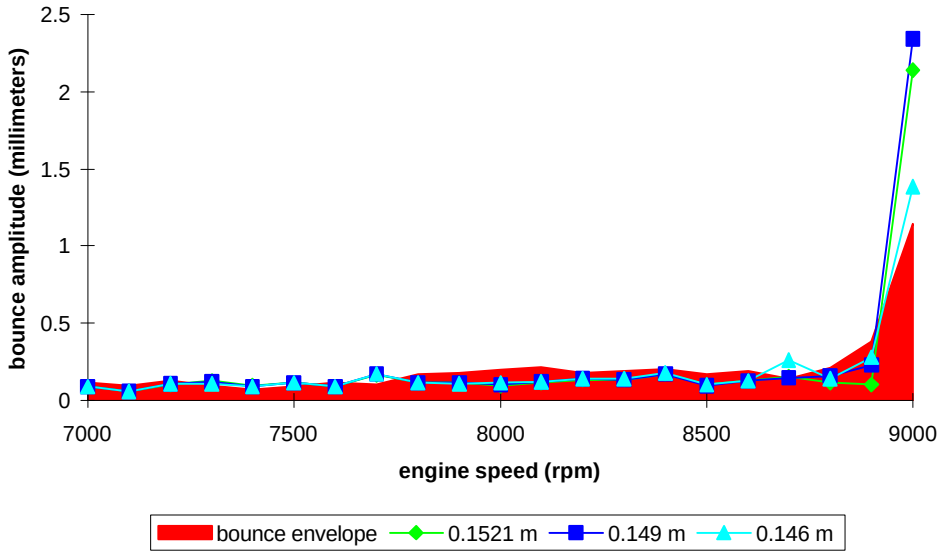

Figure 5.10: Simulated data for the cam generated using various rocker link lengths and the k motion 1600 spring

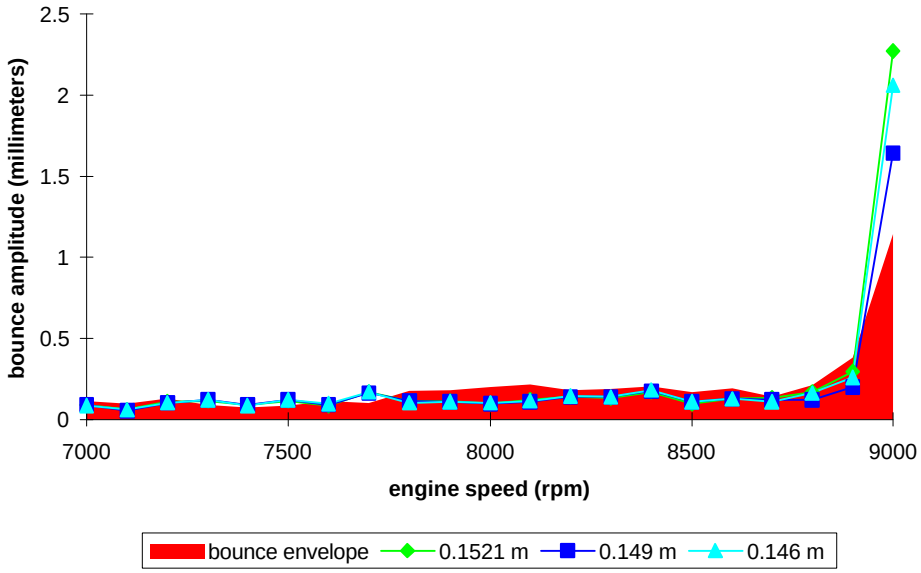

Figure 5.11: Simulated data for the cam generated using various vertical grinding wheel vertical positions and the k motion 1600 spring

5.5 Overview of the CNC Error Investigation

As was discussed above, the simulation of valve train dynamics using cam profiles predicted from changes in the rocker mechanism errors was successful. However, many cam manufacturers now use CNC equipment to manufacture cams. CNC may be used to produce a single prototype or for large production runs. In addition, some of these machines are now equipped with wheel size compensation software to avoid wheel diameter wear pitfalls. Even with this software, errors still occur. As with any machining process, there are inherent errors that result in the manufactured part not being exactly the specified size. However, these parts may still be useful if they lie within a specified tolerance. The tolerance may be as small as 0.00254 millimeters (0.0001 inch) or larger than 0.0254 millimeters (0.001 inch) depending on the machine used to fabricate the part

and its intended purpose. In this investigation, the larger end of the tolerance spectrum for cams will be investigated to determine their effect on the high speed valve train dynamics.

5.6 Actual CNC Error Data

After a cam is manufactured, it is typically measured to check its relationship to the theoretical lift curve. Each lobe is measured and the data recorded as a plot of displacement error versus cam angle. A sample of these traces is shown in Figure 5.12. As can be seen in Figure 5.12, the four error trace plots are dissimilar for each cam position. In addition, even though these errors are the result of a CNC process, they are extreme. Camshaft lift errors are typically on the order of a 0.0050 to 0.0080 millimeters (approximately 2-3 ten thousandths of an inch) when produced on CNC equipment. Some of the errors in Figure 5.12 are almost 10 times that tolerance. It should be noted that the cam error not only effects the lift portion of the cam but the base circle as well. These four error traces will be used to predict their effect on the high speed valve train that was used earlier in this study.

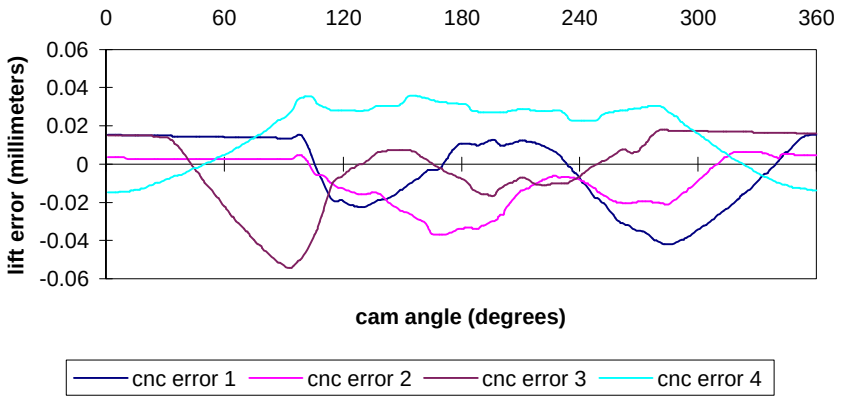

Figure 5.12: Extreme lift curve error from a prototype cam produced on a CNC grinder

5.7 Simulations Using the CNC Grinder Error

In order to investigate the effect of CNC errors on the dynamics of high speed valve trains, the extreme lift error was added to the theoretical cam profile shown in Figure 3.3. In addition, the magnitude of the errors was doubled and the resulting errors were also added to the lift curve to form another set of error lift curves. The lift curves were then differentiated to obtain the velocity curves and the results placed in the simulation.

Simulations were run for both the Comp Cams 938 and K Motion 1600 type springs. The results of the Comp Cams 938 simulations are shown in Figure 5.13 and Figure 5.14 for the original error magnitude and the doubled error magnitude respectively. The results of the K Motion 1600 simulations are shown in Figure 5.15 and Figure 5.16 for the original error magnitude and the doubled error magnitude respectively. The results of the simulations are also plotted along with the bounce envelope of the theoretical valve train setup. As can be seen in each of the figures, both the single and double error magnitudes did not significantly effect the dynamics of the valve train as each of the simulations overlaid each other. The limit speed was also unchanged for each of the simulations. Moreover, most of the bounce amplitudes were within the bounce envelope for each simulation. Even the values that were outside of the bounce envelope were still considered small in terms of valve bounce and are considered acceptable. Therefore, the dynamics of a high speed valve train may not be severely impacted by a large amount of lift error (on the order of thousandths of an inch) when compared to its most stringent tolerances which are on the order of ten thousandths of an inch.

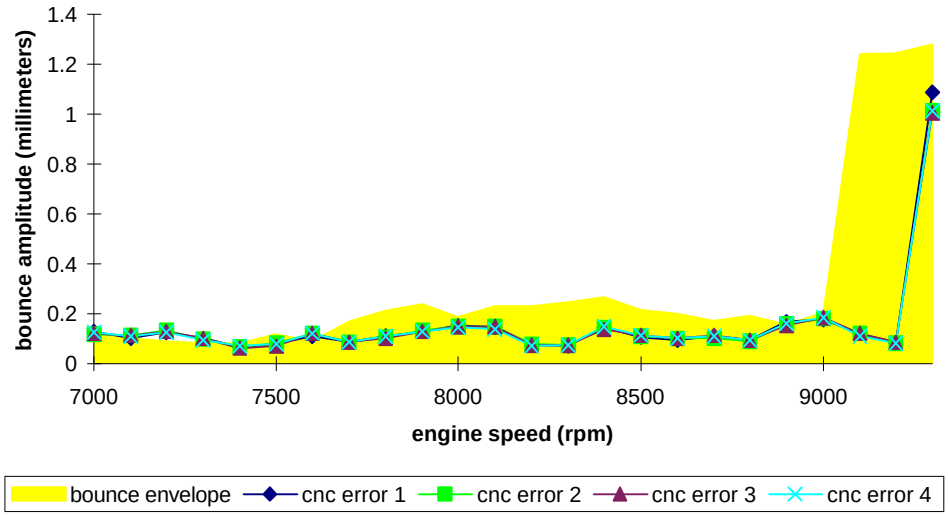

Figure 5.13: Valve train simulation using the four original CNC error plots and the comp cams 938 spring

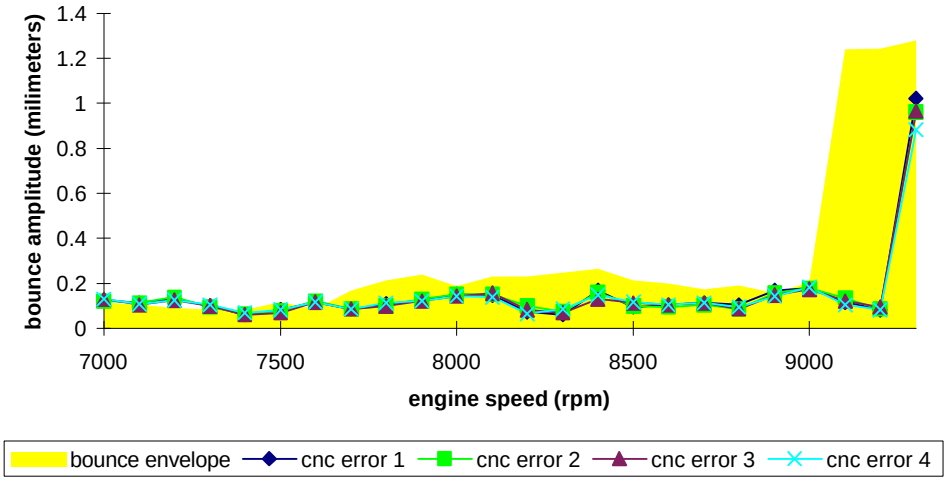

Figure 5.14: Valve train simulation using the four doubled CNC error plots and the comp cams 938 spring

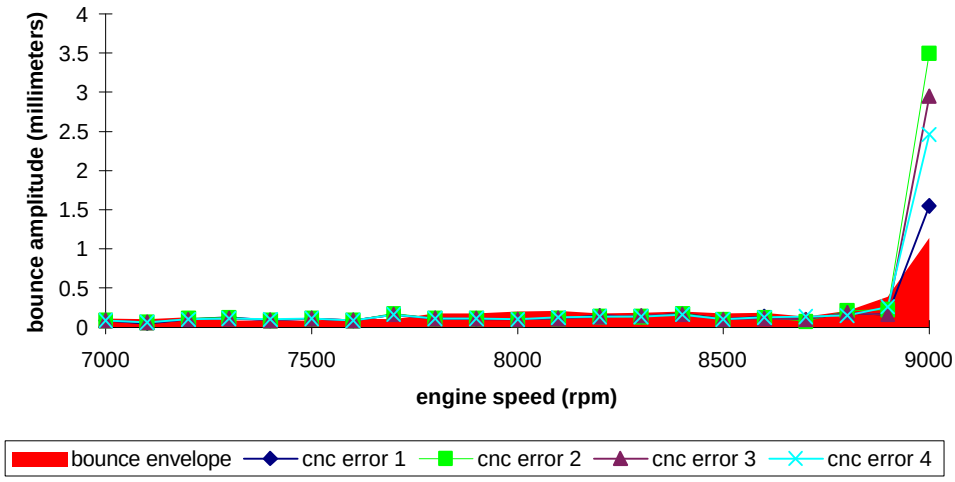

Figure 5.15: Valve train simulation using the four original CNC error plots and the k motion 1600 spring

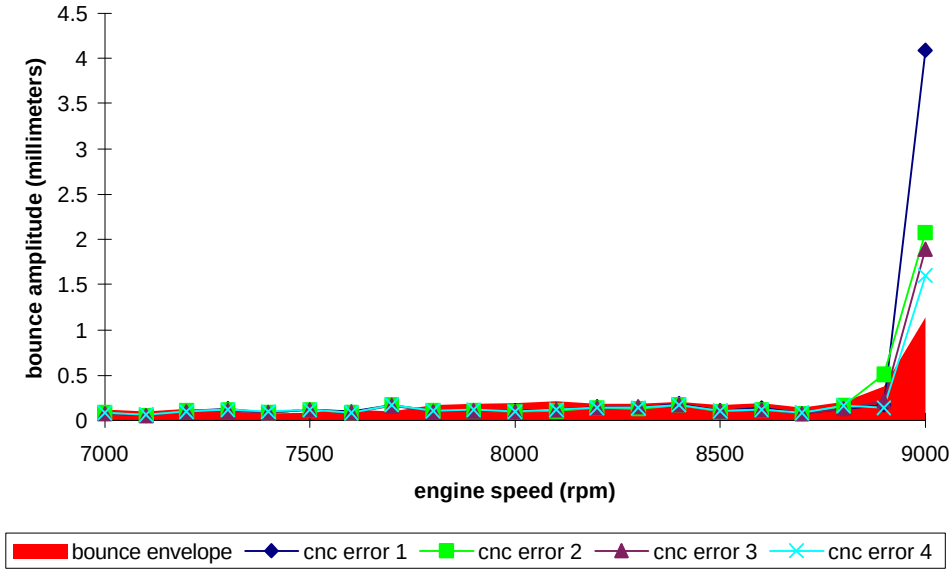

Figure 5.16: Valve train simulation using the four doubled CNC error plots and the k motion 1600 spring